SAE AERO DESIGN REPORT

Northern Arizona University

Aero Jacks Team #327

Carlo Boyd

Ryan Carberry

Luke Chandler

Trey Cooper

Cale Hines

2025-2026

Certification of Qualification

Team Name	NAU AERO JACKS	Team Number	#327
School	NORTHERN ARIZONA UNIVERSITY		
Faculty Advisor	DAVID WILLY		
Faculty Advisor's Email	david.willy@nau.edu		

Statement of Compliance

As faculty Adviser:

DW (Initial) I certify that the registered team members are enrolled in collegiate courses.

DW (Initial) I certify that this team has designed and constructed the radio-controlled aircraft in the past nine (9) months with the intention to use this aircraft in the **2026** SAE Aero Design competition, without direct assistance from professional engineers, R/C model experts, and/or related professionals.

DW (Initial) I certify that this year's Design Report has original content written by members of this year's team.

DW (Initial) I certify that all reused content has been properly referenced and is in compliance with the University's plagiarism and reuse policies.

DW (Initial) I certify that the team shall use the Requirements Check & Safety and Airworthiness Inspection checklists to inspect their aircraft before arrival at Technical Inspection and that the team shall submit the completed checklists, signed by the Faculty Advisor or Team Captain, to the inspectors before Technical Inspection begins.

Signature of Faculty Advisor

2/28/2026

Date

Signature of Team Captain

2/28/26

Date

Note: **A copy of this statement needs to be included in your Design Report as page 2 (Reference Section 4.3)**

Table of Contents

Table of Figures

Table of Tables

TABLE 1: TABLE OF ACRONYMS

Acronym	Definition
SAE	Society of Automotive Engineers
OD	Outer Diameter
ID	Inner Diameter
CG	Center of Gravity
AID	Aircraft Intuitive Design
MAC	Mean Aerodynamic Chord
AOA	Angle of Attach
AOI	Angle of Incidence
FEA	Finite Elemental Analysis

1. Executive Summary

This report illustrates the processes the Northern Arizona University Aero 2-Micro Class team used to design and manufacture a remote-controlled aircraft to compete in the SAE Aero Design West 2026 competition. The design, manufacturing, and testing processes are explained throughout this report. The primary goal of the competition is to manufacture a plane to comply with the SAE rulebook. The design requirements identified for this project can be seen below:

TABLE 2: ENGINEERING REQUIREMENTS

Engineering Requirements	Quantity	Current
Weight Limit	55 [lbs]	7.8 [lbs]
Thrust to Weight Ratio	>0.23	0.513
Takeoff Distance	100 [ft]	30 [ft]
Landing Distance	200 [ft]	150 [ft]
Payload Unload	60 [s]	52 [s]

1.1 System Summary

The aircraft consists of a high-wing monoplane configuration featuring a tricycle landing gear arrangement, dihedral, and a conventional tail. The fuselage is 4.13” OD carbon fiber tube to ensure a structurally sound, yet lightweight design. The wing consists of laser cut balsa Eppler 423 airfoils fastened to 4mm square carbon fiber rods. The dihedral wing shape is achieved by 3-D printed couplers. The empennage consists of laser cut balsa wood NACA 0012 airfoils fastened to 4mm square carbon fiber rod. We constructed a smooth leading edge by gluing cardstock to the front of the airfoils then wrapping with UltraCote. The cardstock leading edge is lighter than a balsa wood leading edge and offers enough rigidity to ensure solid aerodynamic characteristics at the front of the wing. The propulsion system consists of a 1250 kV brushless motor featuring a 12x6.5 2-blade propeller. The team iterated two different airfoils and moved forward with the Eppler 423 airfoil. The electrical circuit

features a 6-axis gyro flight computer, 450-Watt power limiter, a red arming plug and an on/off switch. Figure 1 illustrates the final design which will be brought to Fort Worth.

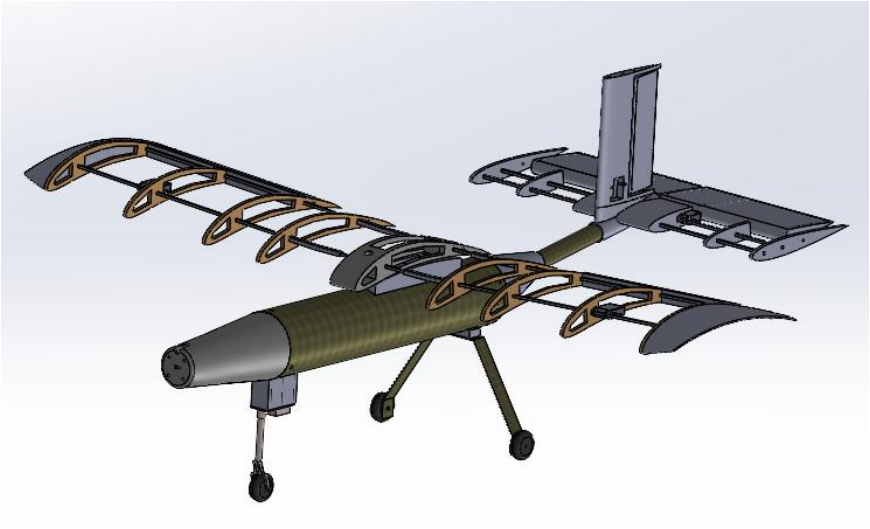

FIGURE 1: FINAL ASSEMBLY

TABLE 3: SYSTEM SUMMARY

Part/Concept	Material	Explanation
Fuselage	Carbon Fiber Tube, OD=4.13" ID=3.995"	Carbon fiber was used for the fuselage because of its high strength-to-weight ratio. The stiffness of the tube allows for consistent mounting and reuse during testing.
Tricycle Landing Gear configuration	Carbon fiber and Aluminum	The tricycle configuration was chosen because of reliable ground control and ease of landing compared to the tail dragger configuration. The nose gear is machined aluminum, and the main gear is carbon fiber.
Wing Foil – Eppler 423	Laser cut Balsa wood	This airfoil selection is explained in later sections.
Spars	4mm square carbon fiber rods	The spars are used to connect and mount the main wing, stabilizers, and wingtips.
Dihedral couplers	3-D printed Bambu Basic PLA	The couplers are 3-D printed to achieve tight tolerance as well as ease of manufacturing. The couplers achieve a 3^{o} dihedral angle giving the plane more stability when rolling. The 9" spar has couplers on both

		ends, then the one 19.5” spar is inserted on both ends to achieve wingspan and correct geometry
Hoerner-like wing tips	3-D printed Bambu Basic PLA	The Hoerner-like wing tips are placed on both ends of the wing. The outermost foil on either side is mounted such that ½” of spar is available to insert the wing tips on. The wing tips increase wingspan collectively by 4”. The wing tips decrease pressure and surface drag, thus enhancing performance
Stabilizer Airfoil – NACA 0012	Laser cut Balsa wood	This airfoil selection is explained in later sections.
Empennage Base	Laser cut Balsa and Bambu Basic PLA	The base of the empennage is 3-D printed due to complex geometry. The component connects the horizontal and vertical stabilizer
Propeller	12x6.5	The team used a dynamometer to test the static thrust of various propellers, and the 12x6.5 propeller with the 450-Watt Power Limiter was found to be the highest thrust.
Wrap	UltraCote	Heat shrink wrap used to encompass outside wing area to provide aerodynamic capability.
1250 kV Brushless Motor	N/A	When coupled with a 12x6.5 propeller, this motor gives ample thrust.
6-axis Gyroscopic flight computer	N/A	The gyroscope helps control the attitude of the airplane by limiting bank and pitch angles.
Red arming plug	N/A	SAE Rulebook Requirement
On/off switch	N/A	SAE Rulebook Requirement
450-Watt Power Limiter	N/A	SAE Rulebook Requirement

1.2 Design Distinction

The carbon fiber fuselage ensures stiff and reliable mounting points. Because of the cylindrical fuselage, the team concluded that 3-D printing mounting components is the best way to ensure consistent, replicable manufacturing as some geometries are quite complex. 3-D printed parts have little lead time

and are iterative because of the low cost and manufacturing time. The team has iterated primarily the nose cone to offer better center of gravity characteristics (CG) by placing the battery inside the nose cone.

2.0 Schedule Summary

The team began this project in September 2025. The first 4 months involved research, calculations and prototyping. Each member of the team was assigned aspects of the plane to research and calculate, those aspects being, main wing, tail, fuselage, electric circuit and landing gear. Following the conducted research, the team began manufacturing and prototyping. The team's Gantt charts can be found in Appendix A – Spring 2026 **Gantt Charts**. At the end of Fall 2025, the team was predominantly focused on prototyping and manufacturing offering little success in terms of flight. As 2026 began, the team conducted new calculations and concluded that a design change was necessary. The primary design change involved switching airfoils and using the Eppler E423 instead of a NACA 2412. The team began testing, iterating, and manufacturing to meet SAE Aero competition requirements.

3.0 Design Layout & Trades

The team created a physical decomposition, seen in Figure 2, outlining all vital subassemblies and their respective parts. This decomposition is important to help the team and stakeholders, and clients understand how the sub-systems work together. It also allows each subassembly lead to understand where their efforts should be focused.

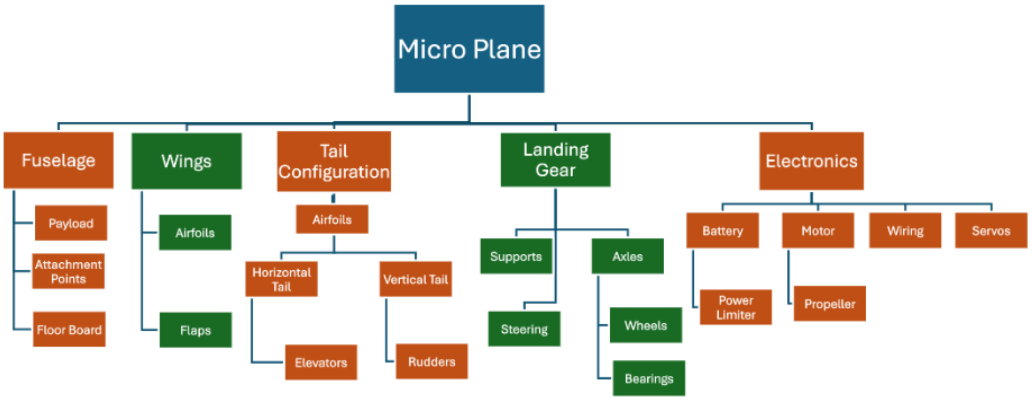

FIGURE 2: PHYSICAL DECOMPOSITION

The electrical circuit consists of two primary branches. The first branch contains a receiver battery which plugs into an on-off switch. The on-off switch then plugs into channel 6 of the receiver. The second branch of the circuit connects a 5,000 mAh lithium polymer battery to our ESC, power limiter, arming plug, and motor.

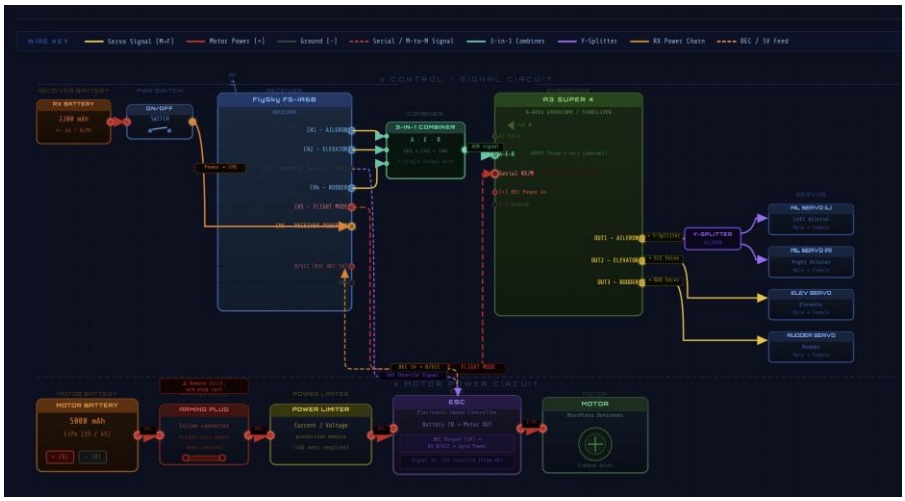

FIGURE 3: ELECTRICAL DIAGRAM

3.1 Overall Design Layout and Size

Table **4** outlines the basic dimensions of the team's airplane, which can be seen in the 2-D Drawing: **Appendix E - 2-D Drawing**.

TABLE 4: PLANE SIZING

Part of Aircraft	Dimension
Wingspan	51 inches
Chord Length	12.6 inches
Wing Area	642.6 inches^2
Main Wing Airfoil	Eppler E423
Empennage Airfoil	NACA 0012
Nose to Tail Length	48.64 inches
Propeller Size	12 x 6.5 inches
Main Gear	6.75 inches
Nose Gear	5.875 inches

3.2 Optimization

Two forms of software were used to provide the team with maximizing flight scores as well as stability. More flight score oriented, a MATLAB code was made to ensure no flight constraints were being seen while maximizing the score. Later in the design process, another code was established to verify and help guide stability principles.

3.2.1 MATLAB-First Iteration

To efficiently create feasible design dimensions, MATLAB was used in creating an optimization code that ran several different parameters against aerodynamic functions such as flight stability and Prandtl coefficients to optimize for the flight score, provided by SAE Aero rulebook [1] seen in Equations 1-3. The MATLAB code was derived from the aircraft optimization code [2], then modified to work with the given constraints and parameters.

$$FS = 3 \cdot W_{Payload} \cdot M + Z \tag{1}$$

$$M = \frac{11}{\left(W_{Empty} - 1\right)^4 + 8.9} \tag{2}$$

$$Z = B_{Takeoff} - S^{1.5} \tag{3}$$

Where $W_{payload}$ is the payload weight (lbs), W_{Empty} is the empty weight (lbs), S is the wingspan (ft), and $B_{takeoff}$ is a score given when the plane takes off, seen below.

$$B_{Takeoff} = \begin{cases} 20 & 0 \leq x \leq 10\ ft \\ 15 & 10 < x \leq 25\ ft \\ 9 & 25 < x \leq 50\ ft \\ 0 & 50 < x \leq 100\ ft \end{cases}$$

The initial parameters used in the code included wing shape, airfoil type, materials, dimensions, payload, velocity, and power. These parameters were then run against different constraints like stability, dimensional interference, center of gravity, and weight to optimize design variables like wingspan, weight of plane, weight of payload, and other dimensions. All optimized variables can be seen in Table 5 which also provides their optimized values based on initial guesses and parameters during the design process thus far, as well as the final iteration with all updated values.

TABLE 5: MATLAB VARIABLES: FIRST AND LAST ITERATION

Symbolic Variable	Physical Quantity	Optimized Value- 1st Iteration	Optimized Value- Final Iteration	Units
P_full	Filled payload weight	1.06E-06	4.53E-06	[lb]
X_p	Payload X location	0.1016	0.4625	[m]
X_w	Wing X location	0.0969	0.380	[m]
b_ht	Horz. tail half span	0.0508	0.2832	[m]
b_vt	Vert. tail half span	0.021	0.1017	[m]
b_w	Wing half span	0.047	0.6477	[m]
c_ht	Horz. tail chord	0.07	0.2238	[m]
c_vt	Vert. tail chord	0.07	0.1300	[m]
cr_w	Wing root chord	0.1663	1.0603	[m]
f_weight	Fuselage weight	14.7884	6.8921	[lb]
l_f	Fuselage length	0.4064	1.1615	[m]
lambda_w	Wing taper ratio	0.9	0.9944	
FS	Flight Score	16.8907	15.7511	

As seen in the maximum flight score, given the initial constraints and parameters, the value came out to 16.8907 in the first iteration, and 15.7511 in the last trial. It is important to note that by flying without a payload, in this case our P_full was zero, that the score cannot be greater than 20. The P_full value being zero is a result of flight stability parameters, where we will have the best possible thrust to weight ratio at the lowest possible weight. The code can be seen in Appendix A.

3.2.2 Stability Optimization

Several resources were used to ensure our aircraft could achieve stable flight. Our team utilized a MATLAB program named Aircraft Intuitive Design Tool (AID) to estimate our Static Margin and the location of our neutral point. Through simulation and experimentation our team concluded that positioning the CG at twenty-five percent of chord resulted in the best performance.

3.3 Design Features and Details (Subassembly Sizing)

All of the materials chosen for the final design were based on their strength, weight and aerodynamic performance. For the fuselage the team decided to go with a circular carbon fiber tube. Carbon fiber has an excellent strength-to-weight ratio allowing for us to have a solid structural base while also remaining as light as possible. By choosing to circular tube this will also help reduce the overall drag the plane will experience allowing for it to be more aerodynamically efficient.

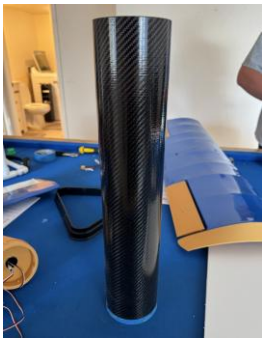

FIGURE 4: CARBON FIBER FUSELAGE

For the spars that support the main and stabilizers, carbon fiber tubing was chose for the same reasons as listed above. The only difference is that the spars are square tubing and this is done so that way the airfoils fit snugly onto them without allowing them to rotate. The ribs for wings and stabilizers are made from laser cut balsa wood. While balsa wood does not have the highest strength it was chosen for how lightweight it is and easy of manufacturing. When properly spaced, the ribs offer adequate rigidity for aerodynamic performance. The last component of the wings was the UltraCote wrap. This is a heat

shrinking wrap which allows it to conform to any design built. The weight of the UltraCote is negligible and ensures proper aerodynamics.

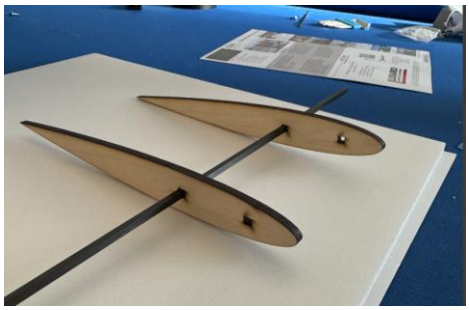

FIGURE 5: BALSA WOOD RIBS AND CARBON FIBER SPARS

For the connecting devices and custom pieces, the team used “Bambu Basic PLA” 3-D print filament. While this filament does not have incredible strength, it was relatively cheap and already optimized for our printing purposes. Having 3-D printing capabilities allowed us to customize our parts based on what we ordered and provided variability.

FIGURE 6: 3-D PRINTED NOSE CONE

Each control surface has a subsequent axis of rotation that is necessary. An extruded cut was modeled on each airfoil allowing a ¼” wooden dowel to be inserted on both sides of each aileron. The elevator utilizes a hollow aluminum rod. The rudder is modeled such that an 1/8” steel rod provides adequate rotation about the vertical stabilizer. Iterating upon manufacturing, it became apparent the tail was too heavy. The team moved away from a 3-D printed elevator and began utilizing Depron.

4.0 Loads and Environments, Assumptions

4.1 Design Loads

The main forces that the airplane needs to withstand are experienced during takeoff, maneuvering, and landing. During takeoff the wings must be able to endure the lift and drag forces that will be present through steep angles of attack. Also, in flight the plane may experience varying turbulent conditions depending on the wind conditions of that day. To combat this the team has designed our wings with a dihedral shape to make the plane more stable along its longitudinal axis. Further down the team talks about the moment that the alerions will produce to make sure the plane will be able to maneuver during flight. The most important force the plane will face will be during landing. To design for the harsh landing stresses, forces the landing gear will have must be estimated. Ultimately, the change in momentum will help us estimate forces given by:

$$F = \frac{m_{aircraft} \cdot \Delta v_y}{\Delta t} \tag{4}$$

However, there must be more calculations completed to find the force. It is assumed that the magnitude of the landing velocity is 53 [ft/s]. If we assume an 8-degree angle of descent (incredibly steep) then we can calculate the velocity in the y-direction given by:

$$v_y = v_{landing} \cdot \sin(\theta) \tag{5}$$

The velocity in the y-direction is calculated to be 7.4 [ft/s]. Now we can calculate the change in momentum. Using a mass of 0.625 [lbm] (10 [lbf]) to ensure a high factor of safety, and our velocity in the y-direction, we can calculate force by using multiple time values. An important note; the smaller the time value, the more intense the landing. The change in time refers to the duration of the pilot's flare. If we consider a time of 0.1 [s] the force is calculated to be 46.25 [lbf]. Now let us consider a time of 0.01 seconds. This is slightly unreasonable, but this way we can visualize how important landing in a controlled fashion is. If we evaluate force at a change in time of 0.01 [s], force will be 462.5 pounds.

This is informative because it shows that decay in force as time increases linearly. This is illustrated in Figure 7.

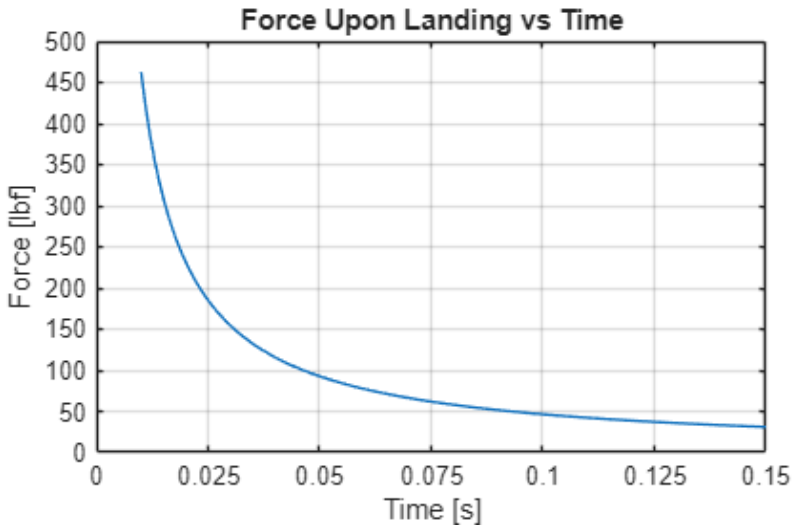

FIGURE 7: FORCE ON LANDING GEAR VS CHANGE IN TIME

4.2 Environmental Conditions

With the team based in Flagstaff, Arizona and the competition being in Fort Worth, Texas, both atmospheric conditions and collected data for projected temperature, pressure, and density were gathered to compare Reynold's numbers at both locations, seen in Table 6.

To calculate Reynolds numbers, Equation 6 was used with the parameters from Table 6, where V is velocity, ρ is density of air, along with chord length of main wing (1.05 feet) for the characteristic length, l.

$$Re = \frac{\rho V l}{\mu} \tag{6}$$

Sutherland's equation, Equation 7 was used to find viscosity, μ where T is temperature, T_0 is reference temperature at sea level, and S is the Sutherland constant.

$$\frac{u}{u_0} = \left(\frac{T}{T_0}\right)^{3/2} \left(\frac{T_0 + S}{T + S}\right) \tag{7}$$

TABLE 6: ENVIRONMENT PARAMETERS

	μ (slug/ft×s)	V (ft/s)	ρ (slug/ft^3)	P (psi)	T(°F)	Re
Flagstaff	3.68E-7	52.5	0.00186	11.3	50	278620
Fort Worth	3.75E-7	52.5	0.00230	14.5	69	338100

5.0 Analysis

5.1 Analysis Techniques

The team used analysis techniques such as MATLAB to perform rough dimensioning analysis to find starting dimensions that yielded acceptable score results from the SAE Aero rulebook. XFLR5 was used on multiple airfoils to find lift and drag coefficients, as well as finding Prandtl's lifting line theorem in three dimensions. SolidWorks was used in all design aspects when creating the subsystems (Fuselage, Main Wing, Empennage, and Landing Gear) as well as FEA analysis of the fuselage and landing gear. SimScale was used for simple FEA structural analysis, specifically on the fuselage. This software-focused analysis allowed for an iterative design process when files were saved and kept in an orderly fashion.

5.2 Performance Analysis

Equations 8 and 9 were used to find lift and drag forces with XFLR5 data for the coefficients of lift and drag of the main wing. The results from these calculations can be seen in the next section through MATLAB plots.

$$L = \frac{1}{2}\,\rho \cdot v^2 \cdot C_L \cdot S \tag{8}$$

$$D = \frac{1}{2}\,\rho \cdot v^2 \cdot C_D \cdot S \tag{9}$$

5.2.1 Takeoff Performance

The team collected taxi data using a stopwatch and cones. The plane covered 75 feet in 2.8 seconds. From this, the acceleration was found to be 19.13 ft/s^2 and a final velocity of 53.57 ft/s. The plane's empty weight is 6.7 pounds. Figure 8 shows the necessary velocity to achieve take-off and the corresponding drag. This was calculated with the 3-D coefficient of lift found at 0^o angle of attack (AoA).

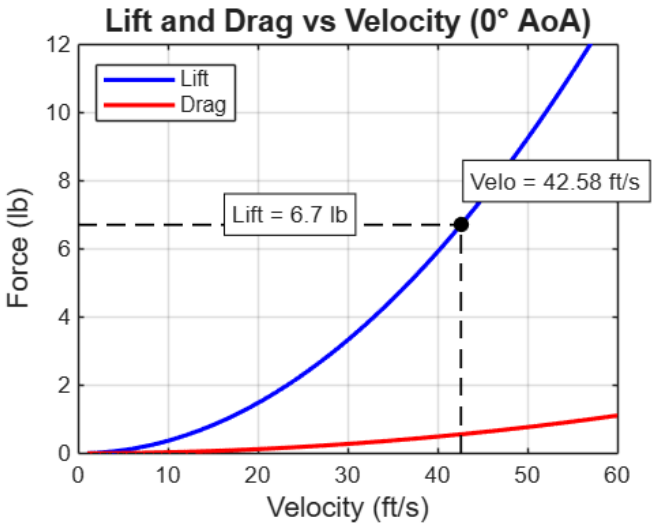

FIGURE 8: LIFT AND DRAG VS VELOCITY (0DEG AOA)

Figure 9 shows the required velocity to achieve takeoff at 3^o AoA. When comparing both figures, it can be easily seen that a higher AoA requires lower velocity to achieve take off.

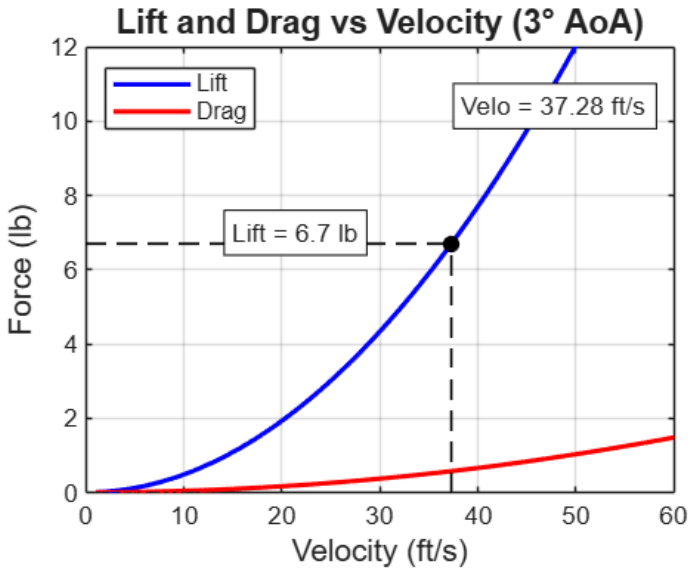

FIGURE 9: LIFT AND DRAG VS VELOCITY (3-DEG AOA)

5.2.2 Main Wing Analysis

When designing a wing, the first step is to find a suitable airfoil for our design constraints. As this competition is located in Fort Worth, Texas, sea level air density was used. The goals of this preliminary analysis were to find and compare lift and drag coefficients at different angles of attack, as well as stall behavior. Initially, the NACA 2412, 2408 0015, and 243024 airfoils were selected and compared using XFLR5, where the choice was clear to move forward with the NACA 2412 airfoil due to its high lift and stall characteristics at around a 15-degree angle of attack.

5.2.3 NACA 2412 Wing Analysis

After selecting the NACA 2412 airfoil, a 3-D straight wing model was created in XFLR5 with dimensions of a 10-inch chord length and 36-inch wingspan. A local drag graph was generated at a Reynolds Number of 300,000 at 20 [m/s]. Figure 10 shows the local drag graph operating at a 10-degree angle of attack. This graph shows a low drag coefficient throughout the wingspan; however, it does spike up at the wing tips, but this is normal due to wingtip vortices.

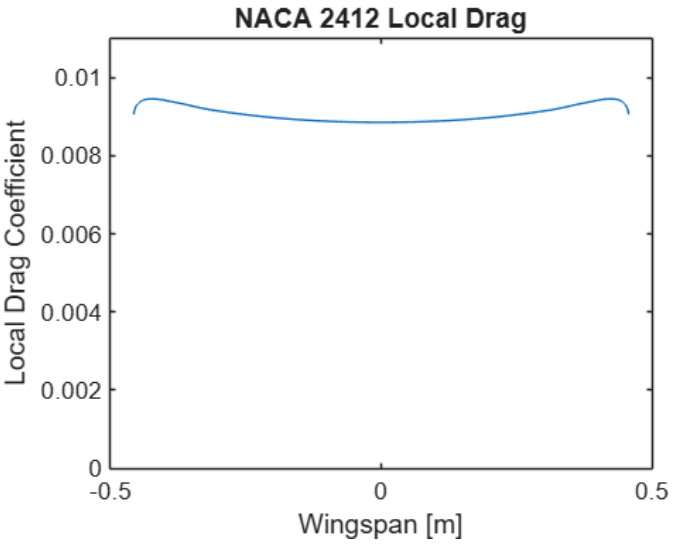

FIGURE 10: NACA 2412 LOCAL DRAG GRAPH

Next, a local lift graph was generated to investigate how the wing will be generating lift at a 10-degree angle of attack. Figure 11 shows that the wings will generate much more lift than drag, which is preferred. The wing is going to generate more lift at the root of the wing, and less lift at each wingtip. While this is a smooth graph and doesn't show any stalling characteristics even at a high angle of attack, exceeding 15 degrees will likely cause the aircraft to stall.

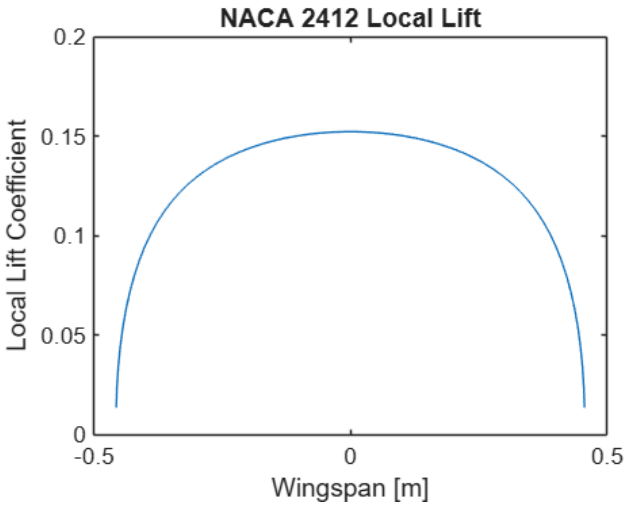

FIGURE 11: NACA 2412 LOCAL LIFT GRAPH

Initially, these results were considered valid, however through field testing, the team found that a ground speed of 20 [m/s] was far too high for analysis and considered switching to a higher-lift airfoil to combat these lower speeds and achieve a smoother take-off.

5.2.4 Eppler 423 Wing Analysis

The team moved forward with the Eppler 423 airfoil, a 51-inch wingspan, and a 12.6-inch chord length, with a 3° dihedral shape. This was then modeled in XFLR5 and ran through the same iterative process as the NACA 2412 airfoil. Figure 12 shows the local drag graph, outlining relatively low drag but high spikes at the wing tips. To combat this, Hoerner-like end caps were designed to gradually decrease skin drag from a previous flat end cap, which limits drag and wingtip vortices.

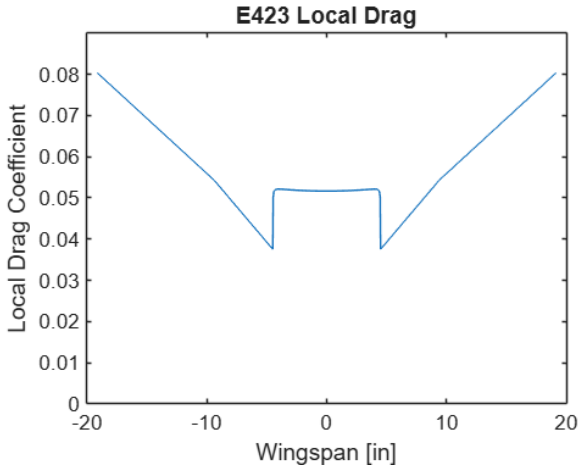

FIGURE 12: E423 LOCAL DRAG VS WINGSPAN

Figure 13 shows the local lift graph of this new wing, outlining a smaller coefficient of lift than the previous wing design, however ground speed decreased in this analysis. The 3° dihedral was implemented to make the wing more stable.

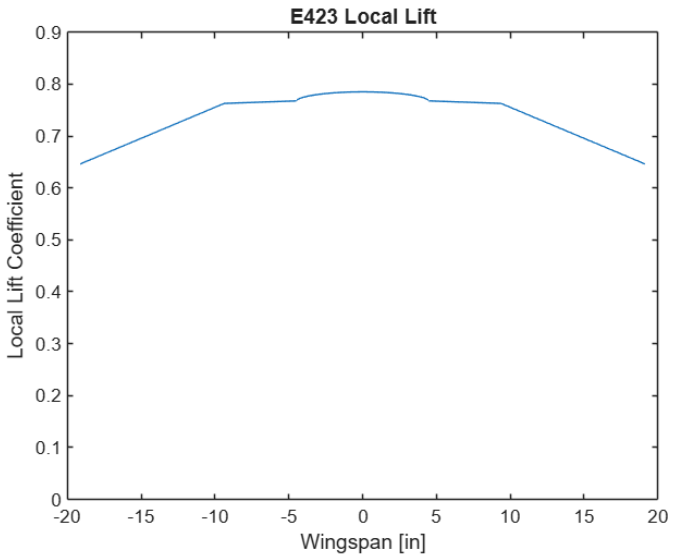

FIGURE 13: E423 LOCAL LIFT GRAPH

Figure 14 shows the three-dimensional coefficient of lift compared to angle of attack. This graph helps the team calculate lift values at takeoff, which was found to be 9º AOA. While the software can produce solutions at high AOA, this AOA (>15º) is typically beyond stall for many airfoils at the Reynolds number of interest because flow separation occurs and the simulation becomes unsteady. XFOIL and VLM/panel approaches are primarily suited to attached or mildly separated flow; thus, results at 15º and beyond should be interpreted qualitatively and should not be used as definitive performance predictions without proper validation.

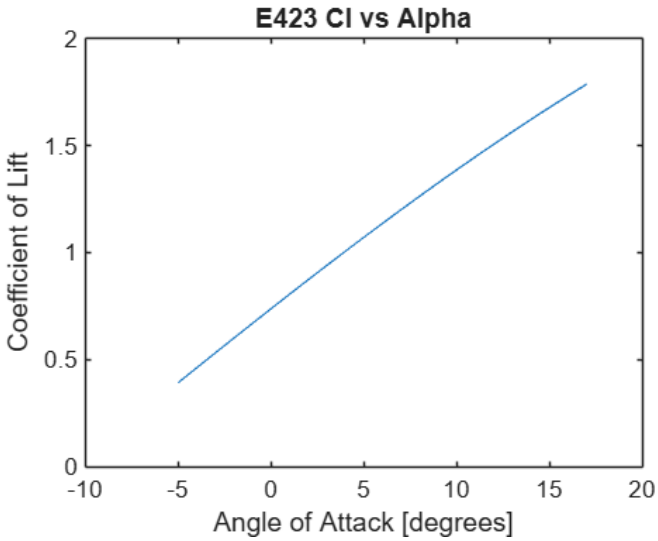

FIGURE 14: 3-D COEFFICIENT OF LIFT VS. ALPHA

When designing the ailerons for the wing, finding a dynamic moment will show how effective the ailerons are at producing roll.

TABLE 7: VARIABLES AND VALUES FOR AILERON DYNAMIC MOMENT

Variable:	Description:	Value:
$C_{l\varepsilon}$	Aileron lift increase with deflection angle (ε)	0.03837
$C_{l\alpha}$	Lift coefficient at 0° AOA	0.74
γ	Aileron chord length	3.75 [in]
$S_{aileron}$	Surface area of aileron	45 [in^2]
S_{ref}	Wing area	642.6 [in^2]
$y_{aileron}$	Spanwise center of aileron (center of aileron → wing root)	19.5 [in]
b	Wingspan	51 [in]
ε	Deflection angle	(±3, ±5, ±7)° [convert to rad]
q_∞	Dynamic pressure	0.223 [$\frac{lb}{in^2 \times s}$]
M	Dynamic moment	(±14.7, ±24.5, ±34.3) [$\frac{lb \times in}{s}$]

Equation 10 was used to find the Aileron lift increase with deflection angle of our ailerons. This calculation was performed with the lift coefficients at a 0° angle of attack to simulate roll cruising flight.

$$C_{l\varepsilon} = C_{l\alpha} \times \sqrt{\gamma} \times \frac{S_{aileron}}{S_{ref}} \times \frac{y_{aileron}}{b} \tag{10}$$

Equation 11 was then used to find the dynamic moment at deflection angles of ±3, ±5, and ±7°. The values came out to ±14.7, ±24.5, and ±34.3 [$\frac{lb \times in}{s}$]. As the plane weighs around 7.8 pounds, we shortened the throw and sensitivity of the controls to keep from over rotating when roll is produced.

$$M = C_{l\varepsilon} \times \varepsilon \times S_{ref} \times b \times q_\infty \tag{11}$$

5.2.5 Empennage Analysis

Information obtained from the main wing design, such as the Reynolds number, helps to guide empennage design decisions. To narrow down the selections, XFLR5 is used once again. After doing

research on empennage design, three NACA airfoils were selected to compare the different features they had. Figure 15 shows the relation between the coefficient of lift to the coefficient of drag at the angles of attack. The symmetric airfoils, 0009 and 0012, display similar results which start to fluctuate at the larger angles of attack. The NACA airfoil 6409 has a camber, meaning it will generate higher lift at all angles of attack without producing much drag.

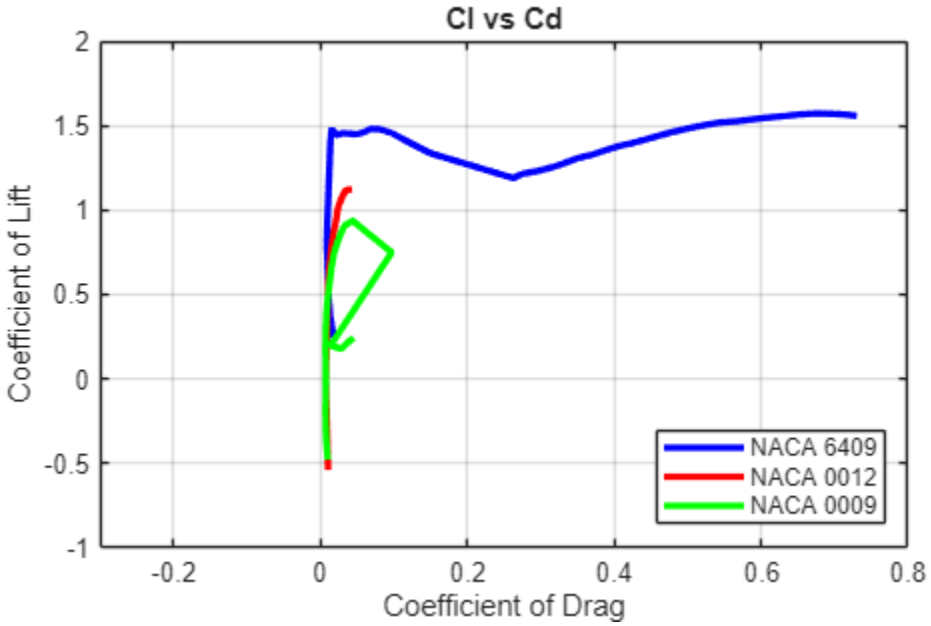

FIGURE 15: COEFFICIENT OF LIFT VS COEFFICIENT OF DRAG

Figure 16 shows a similar trend as observed above with the fact that the cambered airfoil once again starts to produce higher lift coefficients all the way through; however, in regard to the NACA 6409 (Blue lines) and NACA 0009 (Green lines) at higher angles of attack, the graphs begin to deviate from the linear path, indicating signs of stalling. Selecting a wing that stalls at a higher angle of attack reduces the risk of a crash on takeoff.

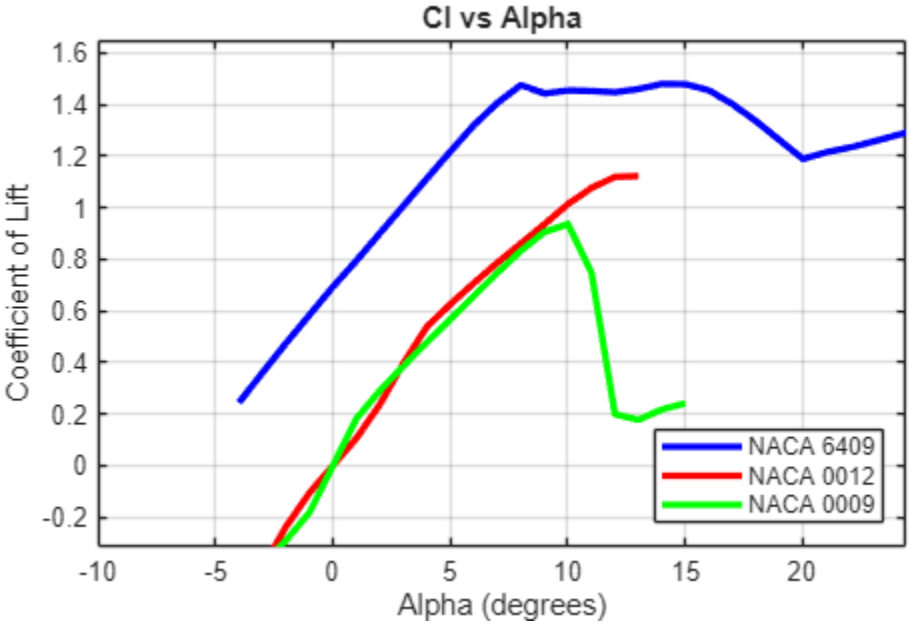

FIGURE 16: COEFFICIENT OF LIFT ACROSS INCREASING ANGLES OF ATTACK

The final parameter in design decisions for the empennage is the pitching moment, seen in Figure 17. Based on research from relevant aerodynamic sources [3], symmetrical airfoils were found to be the most suitable choice for the application. If the empennage is to produce a negative pitching moment, the main wing must be able to produce excess lift to keep the aircraft level. With much larger planes this is not a problem but since handling and stability are more sensitive for RC aircraft, this would create issues. Reducing the negative pitching moment allows for more control and stability in the air. From results in the figures, the NACA 0012 airfoils were selected for their ideal characteristics: small pitching moment, linearity for lift, and small amounts of drag.

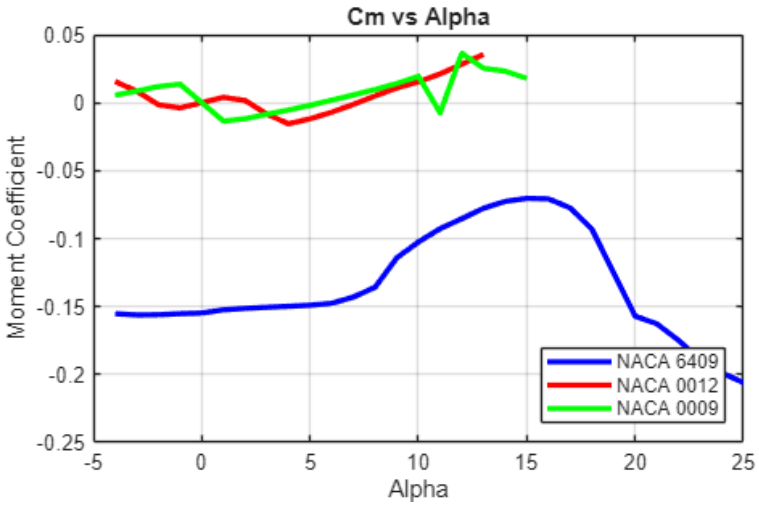

FIGURE 17: PITCHING MOMENT ACROSS INCREASING ANGLES OF ATTACK

5.3 Structural Analysis

5.3.1 Fuselage Analysis

The initial fuselage design included four cutout hatches to allow for quick access to all electronics and hardware. Although this analysis proved the fuselage to be structurally sound with all hatches, the team decided to eliminate them. This elimination allowed for a quicker and simpler manufacturing process, as hatches are difficult to manufacture and don't have consistent replicable geometry. Eliminating the hatches also eliminated the need for any excessive hardware, in turn ridding the plane of extra weight. This new fuselage design also proved to be more structurally sound, seen in Figure 18. The maximum deflection, with 250 lbs of force on each landing gear, shows that maximum deflection is .002394in, proving the fuselage to be structurally sound.

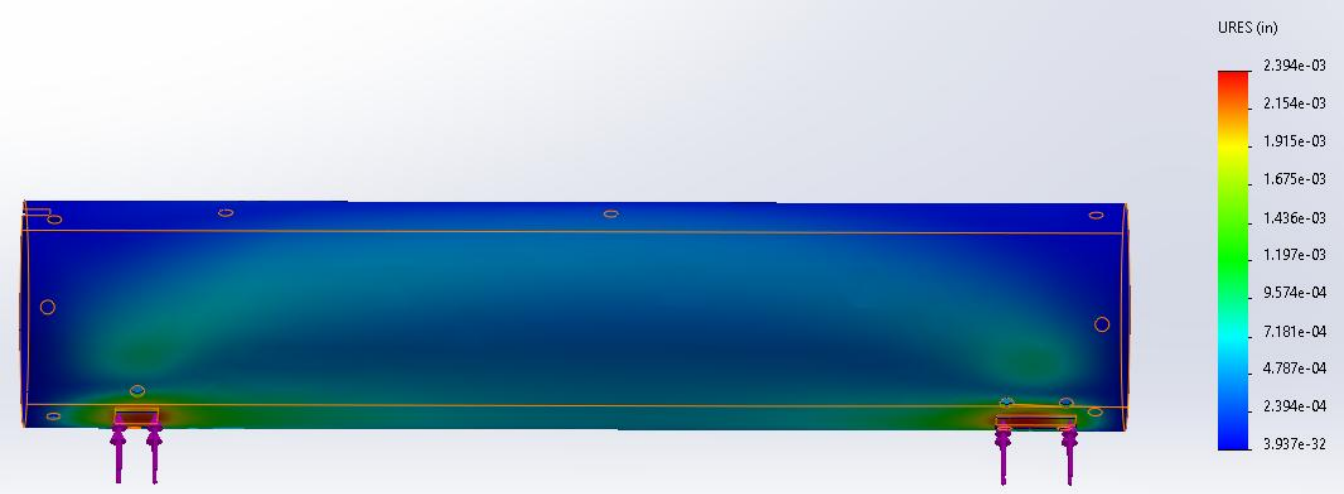

FIGURE 18: FUSELAGE FEA

6.0 Assembly & Sub-Assembly, Test and Integration

This section details sub-assemblies, their design, and how testing was achieved. The main wing, along with empennage, had respective printed parts to attach to the main fuselage. All assemblies were optimized for the best possible flights in terms of stability.

6.1 Wing Assembly and Integration

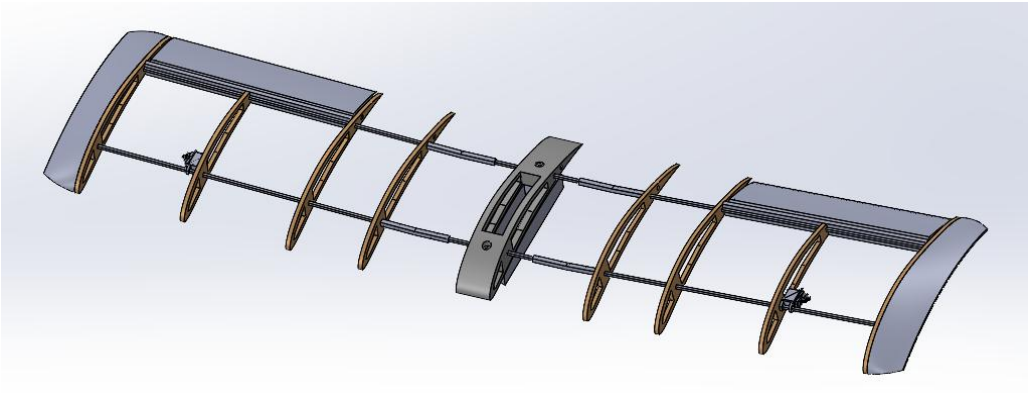

FIGURE 19: WING SKELETON

The main wing sub-assembly is built as one continuous part and is integrated into the fuselage with two 10-32 bolts, one is 2 inches long and the other is 1.5 inches. The bolts are fastened with two 10-32 lock-nuts, against a 3-D printed mounting airfoil and 3-D printed mounting plate, mirroring the airfoil shape and fuselage curve on the bottom.

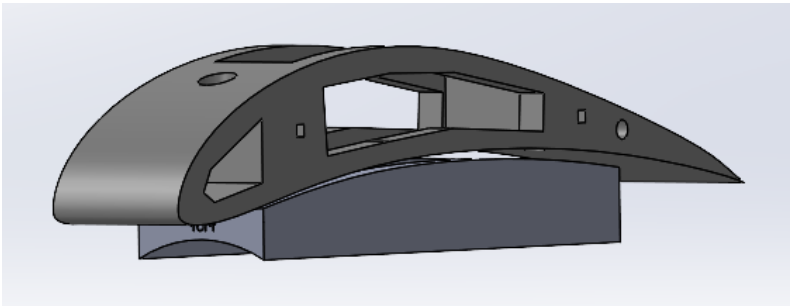

FIGURE 20: MOUNTING AIRFOIL AND MOUNTING PLATE

Using a CG stand and the Aircraft Intuitive Design Software, we calculated that our aircraft would have a static margin of 27%. Through flight testing, this static margin was found to perform the best.

The wing implements two MG90 servos for aileron control, mounted internally using a 3D printed servo mount connecting to the front spar. Control arms and horns are connected externally to the ailerons.

The servos are wired internally to a splitter cable, threaded through the mounting plate into the fuselage, which is connected to our gyro, lastly feeding to the receiver. These servos are mounted in a way that enables the ailerons to deflect in opposite directions.

6.2 Fuselage and Empennage Integration

The fuselage is a carbon fiber cylinder with an inner diameter of 3.995”. From the back end of this extends the boom which is Kevlar reinforced carbon fiber. The boom connects the empennage to the rest of the plane using a 3-D printed device. Three nut inserts were placed into this boom connector so the team can drill into the fuselage, creating a secure connection with machine screws. The boom then slides into the connection at a 10° angle, originally at 7.25°, to bring the empennage level with the main wings; therefore, eliminating downwash it may experience if it was placed below the main wing. The angle was increased to 10° so during takeoff it has more degrees of rotation upwards without encountering a tail strike. To connect the empennage to the boom another 3-D printed part was designed as a empennage adapter, where the airfoil for the horizontal stabilizer was given a -3° angle of incidence, so that the empennage can produce a natural downward aerodynamic force to counter the moment produced by lift of the main wing.

FIGURE 21: FULL FUSELAGE ASSEMBLY

6.3 Landing Gear and Control System

The nose gear has an external servo mount thus creating space inside the fuselage for other electrical controls and servo cables. The nose gear and rudder are both wired to a splitter cable to move in tandem achieving maneuverability. The main gear is a purchased carbon fiber model.

6.4 Testing and Validation

To ensure stable flight, all systems went through a respective testing procedure. A pre-flight checklist was used in order to ensure all electrical and mechanical systems worked properly and reduce the risk of crash. Performance of the aircraft was validated through flight tests.

6.4.1 Control Surface Calibration

The original prototype the team designed had control surfaces on the empennage that were too small and could not adequately fit the needed parts. Since this oversight into design, the team has redesigned to ensure that all servos and linkage rods have the proper rotation and reliability. The team has programed the servos with varying throw percentages and sensitivity to obtain superior in-air control and stability.

FIGURE 22: CONTROL SURFACE TESTING

6.4.2 Electrical System and Thrust Testing

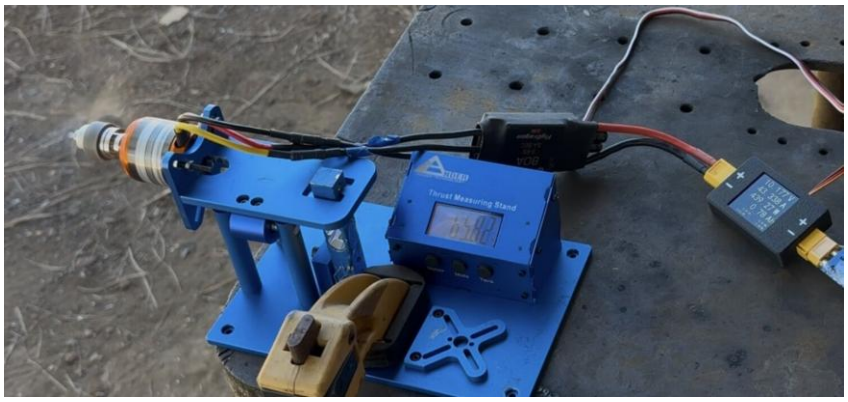

FIGURE 23: STATIC THRUST TESTING

The electrical components for our aircraft were selected in a systematic way to achieve certain design goals. Our airplane utilizes a 1250 kV Motor and a 12 x 6.5 inch propeller. This configuration enabled us to produce 4 lbs of static thrust, during dynamometer testing; resulting in a static thrust to weight ratio of 0.597. Great care was also taken to ensure our system was capable of handling all expected loads during flight. The electrical components were expected to draw a total maximum of 72 Amps at full load. An 80 Amp ESC was integrated into the circuit to provide our team with a factor of safety of 1.1. Our 5,000 mAh battery also provides our team with 6 minutes of flight time while not exceeding a depth of discharge of 80%.

7.0 Manufacturing

This Section outlines how all subassemblies were manufactured through the engineering process; a full manufacturing plan can be seen in **Appendix D – Manufacturing Plan**.

7.1 Fuselage

The fuselage was designed with a 20 inch long, 4-inch ID carbon fiber tube. A 3-D printed jig was created for repeatability between the different fuselages. This jig included 3 pieces attached to a square

rod, with the middle piece not secured in order to create top and bottom lines on the cylinder. The frontmost jig contained three pilot holes for the nose cone connection, and four holes for the main gear, all dimensioned through SolidWorks according to the final assembly. The middle section contained one top hole that would be used for the front and back of the wing mount, as well as two bottom holes used for the rear main gear. The back jig piece had three holes for the boom connector attachment as well as a top notch for the centerline coming off the boom connector. For the on/off switch and red arming plug, two notches were cut to size 3” in front of the leading edge to not interfere with the bladder below.

FIGURE 24: FUSELAGE WITH JIG ATTACHMENTS

7.1.1 Bladder

For the bladder the team decided to go with a 3-D printed design that will be sealed with a polyurethane spray for its watertight properties. Then center of gravity of the bladder will be in line with the center of gravity of the plane. This is done purposely so the team does not have to worry about having differing centers of gravity with an empty versus a full payload. Two bolts were 3-D printed to thread into preset nuts into the bladder, these bolts were also given o-rings to keep a watertight seal with a full bladder.

FIGURE 25: CROSS SECTION OF BLADDER

7.1.2 Main Wing

The wing assembly includes eight balsa wood cut E423 airfoils, one 3-D printed mounting airfoil, a 3-D printed mounting plate, two 4mm square by 9-inch carbon fiber struts, four 4mm square by 19.5-inch carbon fiber struts, four 3-D printed couplers with a 3° angle from the horizontal, and two 3-D printed Horner-like end caps. All 3-D printed parts were printed out of Bambu Basic PLA at varying infills. The wing implements cardstock for the leading edge and supports throughout the middle of the wing, as well as thin balsa wood for a trailing edge. UltraCote was used with a wrapping iron and a heat gun to tac and finish. The wings are built as one complete part, and are mounted on the top of the fuselage with two bolts and nuts connecting the mounting foil to the mounting plate and the fuselage as seen in Figure 20.

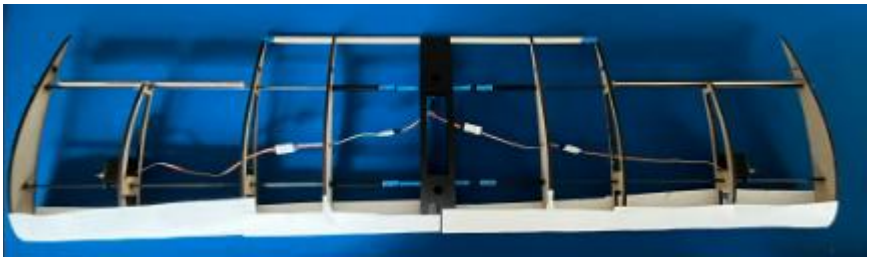

FIGURE 26: WING SKELETON

The top mount was decided over a side fuselage mount with two half-wings for ease of manufacturability as our fuselage is a cylinder. The wings are mounted parallel to the fuselage, however the landing gear is configured such that the wings are at a 3.3189° angle of incidence relative to the

ground. This angle of incidence allows our plane to produce lift while keeping our fuselage parallel to the airflow, thus reducing drag.

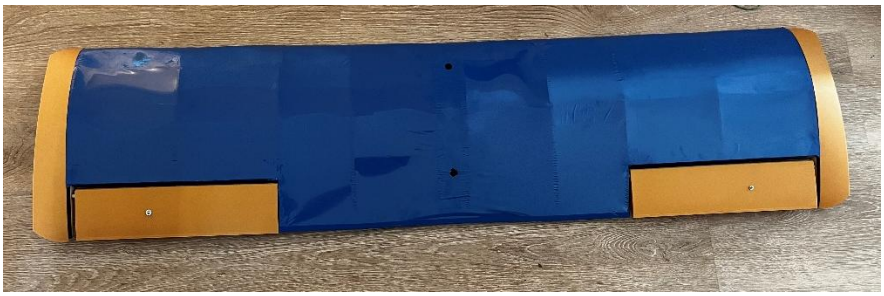

FIGURE 27: MANUFACTURED MAIN WING

7.1.3 Empennage

The empennage was manufactured with ¼” balsa wood airfoils, 4 mm carbon fiber square tubing, 3-D designed parts, UltraCote, Depron foam, aluminum rod and cardstock. The 3-D printed tail adapter connected onto the boom with basic airfoil shapes to allow quicker and more accurate manufacturing. Two spars that were cut to length are inserted into each side of the connecting device, and in turn support the airfoils and servo mounts. Six balsa wood airfoils (NACA 0012) are used to give the wing its shape. Four of these, placed in the middle, are cut to be flush with the connecting device to not interfere with the elevator. Once the ribs are located on the correct spots, superglue is applied to the spars ensuring proper adhesion. To help reduce drag, servos were mounted internally in the horizontal and vertical stabilizer. A leading edge constructed out of cardstock was glued on to the balsa wood ribs, helping both aerodynamic properties and to give better adhesion when wrapping the wing in UltraCote. Once the glue had been given an adequate time to dry the two sides of ribs and spars were removed from the connecting device to be wrapped. This was done so that way the parts are easily interchangeable if anything breaks. The vertical stabilizer and rudder were both 3-D printed, due to the small size this would give us the easiest manufacturing and lowest weight. These were also held in by the carbon fiber spars and a steel rod to allow for the rudder to rotate. Finally, an elevator made of Depron foam was constructed and connected to the horizontal airfoils also with aluminum rods. All of these manufacturing

decisions were made through trial and error with goals of optimizing weight and aerodynamic performance.

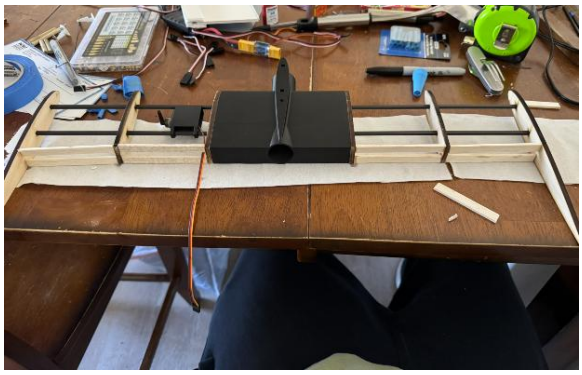

FIGURE 28: SKELETON VIEW OF EMPENNAGE

FIGURE 29: WRAPPED HORIZONTAL STABILIZER

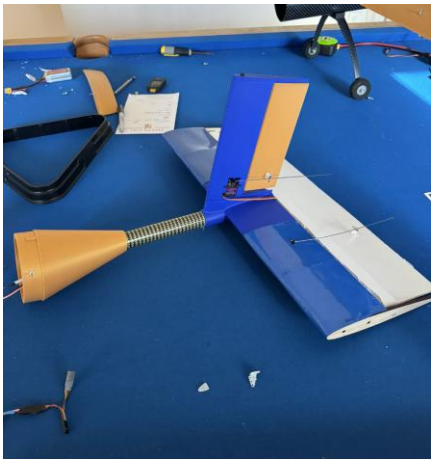

FIGURE 30: FULLY ASSEMBLED EMPENNAGE

8.0 Conclusion

The Northern Arizona University AeroJacks has completed many iterations in manufacturing, design, analysis and testing. The plane consists of a high wing design consisting of a cylindrical fuselage. The wing features E423 airfoils and carbon fiber spars reaching a wingspan of 51”. The empennage is attached via carbon fiber boom and is made up of a 3-D printed adapter and NACA 0012 airfoils reaching 22.3” in span. The bladder is 3-D printed to achieve and work around complex geometry within the fuselage. Our team believes our aircraft will fly stably and meet the requirement of delivering the 2L payload.

9.0 References

[1] SAE, *2026 Collegiate Design Series SAE Aero Design Rules,* SAE, 2026.

[2] MATLAB, "Aircraft Design Optimization with Fixed Wing Object," MATLAB, 2025. [Online]. Available: https://www.mathworks.com/help/aerotbx/ug/aircraft-design-optimization-with-the-fixed-wing-object.html. [Accessed 16 October 2025].

[3] J. D. Anderson, Aircraft Preformance and Design, Boston: McGraw-Hill Higher Education, 2012.

[4] P. R. Nick Slusher, "Introduction to XFLR5," Notre Dame University, Notre Dame, 2023.

[5] "Airfoil Tools," 2026. [Online]. Available: http://airfoiltools.com/. [Accessed 2025-2026].

[6] "Principles of Flight," cfinotebook, [Online]. Available: https://www.cfinotebook.net/notebook/aerodynamics-and-performance/principles-of-flight. [Accessed 14 September 2025].

[7] "Design and Analysis Notes," RC Aero Notes, 21 January 2017. [Online]. Available: https://rcaeronotes.wordpress.com/design-and-analysis-notes/. [Accessed 14 September 2025].

[8] A. Wood, "Horizontal and Vertical Tail Design," AeroToolbox, 25 June 2017. [Online]. Available: https://aerotoolbox.com/design-aircraft-tail/. [Accessed 20 October 2025].

Appendix A – Spring 2026 Gantt Charts

Task Mode	Task Name	Duration	Start	Finish	Resource Names	Predecessors	Succ
	Week 1	**5 days**	**Tue 1/13/26**	**Sun 1/18/26**	**Week1**		
	Staff meeting #1	1 day	Tue 1/13/26	Tue 1/13/26	SM#1		3
	Get started on prototype 4	4 days	Wed 1/14/26	Sun 1/18/26	Begin Manufacturing	2	5,4
	Week 2	**6 days?**	**Mon 1/19/26**	**Sun 1/25/26**		**3**	
	Timecard Wk 1	1 day	Mon 1/19/26	Mon 1/19/26	Turn in TC#1	3	6
	Staff meeting #2	1 day	Tue 1/20/26	Tue 1/20/26	SM#2	5	7
	Finish Proto 4	4 days	Wed 1/21/26	Sun 1/25/26	S26 Pr1 Complete	6	8,9
	Week 3	**6 days?**	**Mon 1/26/26**	**Sun 2/1/26**		**7**	
	TimeCard Wk 1	1 day	Mon 1/26/26	Mon 1/26/26	Turn in TC#2	7	10
	Staff Meeting #3	1 day	Tue 1/27/26	Tue 1/27/26	SM#3	9	11
	Start Proto 5	4 days	Wed 1/28/26	Sun 2/1/26	S26 Pr2 start	10	12,1
	Week 4	**6 days?**	**Mon 2/2/26**	**Sun 2/8/26**		**11**	
	Timecard Wk 3	1 day	Mon 2/2/26	Mon 2/2/26	Turn in TC#3	11	14
	Staff Meeting #4	1 day	Tue 2/3/26	Tue 2/3/26	SM#4	13	15
	Finish Proto 5	4 days	Wed 2/4/26	Sun 2/8/26	S26 Pr2 Complete	14	16,1
	Week 5	**6 days?**	**Mon 2/9/26**	**Sun 2/15/26**		**15**	
	Timecard Wk 4	1 day	Mon 2/9/26	Mon 2/9/26	Turn in TC#4	15	18
	100% Hardware Status Update	1 day	Tue 2/10/26	Tue 2/10/26	100% Hardware Presentation in	17	19
	Begin 2-D drawings for SAE	4 days	Wed 2/11/26	Sun 2/15/26	Start 2-D Drawings for SAE	18	20,21
	Week 6	**6 days?**	**Mon 2/16/26**	**Sun 2/22/26**		**19**	
	Timecard Wk 5	1 day	Mon 2/16/26	Mon 2/16/26	Turn in TC#5	19	22
	Staff Meeting #5	1 day	Tue 2/17/26	Tue 2/17/26	SM#5	21	23
	Make any adjustments needed to Proto 5 and drawings	4 days	Wed 2/18/26	Sun 2/22/26		22	24,25

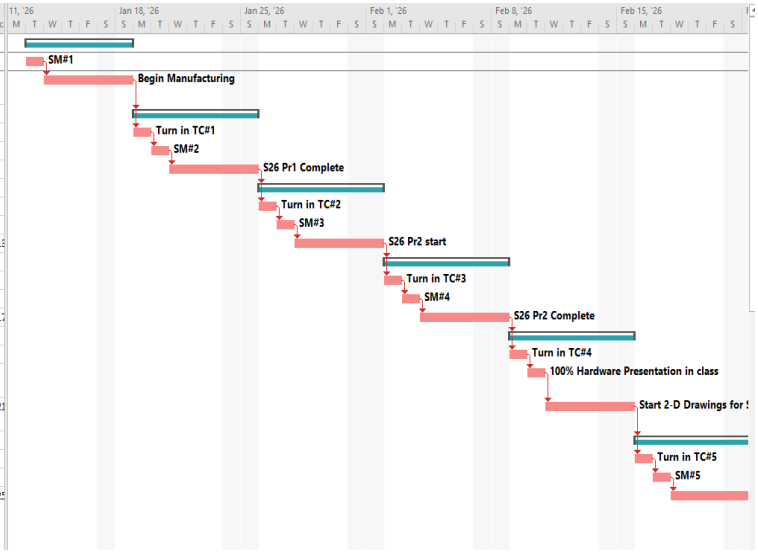

FIGURE 31: SPRING GANTT CHART WEEKS 1-6

Task Mode	Task Name	Duration	Start	Finish	Resource Names	Predecessors	Succ
	Week 7	**6 days?**	**Mon 2/23/26**	**Sun 3/1/26**		**23**	
	Timecard Wk 6	1 day	Mon 2/23/26	Mon 2/23/26	Turn in TC#6	23	26
	Staff Meeting #6	1 day	Tue 2/24/26	Tue 2/24/26	SM#6	25	27
	Submit SAE 2D drawings, Technical Data Sheet and Technical Design Report	3 days	Wed 2/25/26	Fri 2/27/26	Big SAE Aero Submission	26	28
	Begin work on 66%+ Hardware update	1 day	Sun 3/1/26	Sun 3/1/26	Work on capstone class submission	27	29,30
	Week 8	**6 days?**	**Mon 3/2/26**	**Sun 3/8/26**		**28**	
	Timecard Wk 7	1 day	Mon 3/2/26	Mon 3/2/26	Turn in TC#7	28	31
	Give 66% update	1 day	Tue 3/3/26	Tue 3/3/26	66% Update	30	32
	Continue workin on Prototype	2 days	Wed 3/4/26	Thu 3/5/26	More Proto	31	33
	Spring Break	12 days	Fri 3/6/26	Sun 3/22/26	Spring Break	32	34,35
	Week 9	**6 days?**	**Mon 3/23/26**	**Sun 3/29/26**		**33**	
	Timecard Wk 8	1 day	Mon 3/23/26	Mon 3/23/26	Turn in TC#8	33	36
	Staff meeting #7	1 day	Tue 3/24/26	Tue 3/24/26	SM#7	35	37
	Practice Flying	4 days	Wed 3/25/26	Sun 3/29/26	Flight Practice	36	38,39
	Week 10	**6 days?**	**Mon 3/30/26**	**Sun 4/5/26**		**37**	
	Timecard Wk 9	1 day	Mon 3/30/26	Mon 3/30/26	Turn in TC#9	37	40
	Staff meeting #8	1 day	Tue 3/31/26	Tue 3/31/26	SM#8	39	41
	Poster draft	3 days	Wed 4/1/26	Fri 4/3/26	Poster Draft	40	42
	Flight Practice	2 days	Sat 4/4/26	Sun 4/5/26	Flight Practice	41	43,44

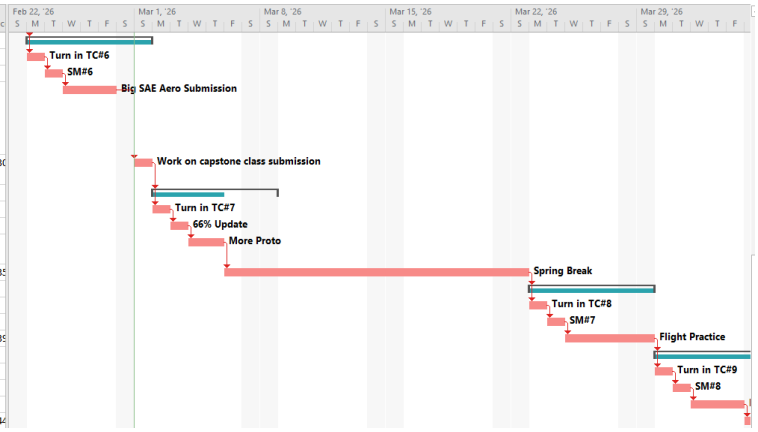

FIGURE 32: SPRING GANTT CHART WEEKS 7-10

	Week 11	**6 days?**	**Mon 4/6/26**	**Sun 4/12/26**		**42**	
	Timecard Wk 10	1 day	Mon 4/6/26	Mon 4/6/26	Turn in TC#10	42	45
	100% Hardware Presentation	1 day	Tue 4/7/26	Tue 4/7/26	Hardware Presentation in	44	46
	Flying!!!!	4 days	Wed 4/8/26	Sun 4/12/26	Flight Practice	45	47,48
	Week 12	**6 days?**	**Mon 4/13/26**	**Sun 4/19/26**		**46**	
	Practice Flying	3 days	Mon 4/13/26	Wed 4/15/26	More Flight Practic	46	49
	Leave For Competition	1 day	Thu 4/16/26	Thu 4/16/26	Drive to DFW	48	50
	Compete and WIN	2 days	Fri 4/17/26	Sun 4/19/26	WIN THE DANG THI	49	51
	Capstone Completed	16 days	Mon 4/20/26	Sun 5/10/26	We HAVE WON AT	50	

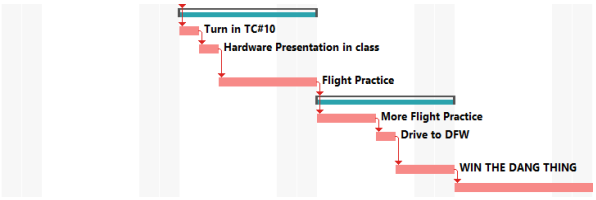

FIGURE 33: SPRING GANTT CHART WEEKS 11-12

Appendix B - MATLAB Optimization

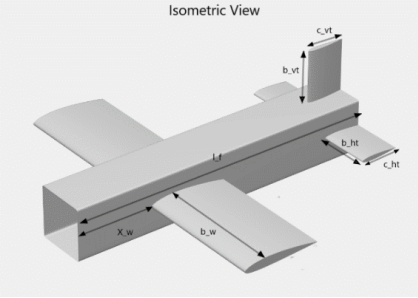

Symbolic Variable	Physical Quantity	Units
P_full	Filled payload weight	[lb]
X_p	Cargo X Location	[m]
X_w	Wing X Location	[m]
b_ht	Horz. Tail half span	[m]
b_vt	Vert. Tail half span	[m]
b_w	Winghalf span	[m]
c_ht	Horz. Tail Chord	[m]
c_vt	Vert. Tail chord	[m]
cr_w	Wing root chord	[m]
f_weight	Fuselage weight	[lb]
l_f	Fuselage Length	[m]
lambda_w	Wing taper ratio	

```
% Define Constants and Optimization Values
[aircraft, wing, fuselage, hTail, vTail, payload, initialValues] = initializeAircraft;


% Setup Design Problem
designprob = optimproblem('ObjectiveSense','maximize');


% Estimate lift and drag coefficients for the wing, tail, and fuselage
[aircraft, wing, fuselage, hTail, vTail, designprob] = ...
    addAerodynamics(aircraft, wing, fuselage, hTail, vTail, designprob);


% Use the component build-up method to formulate the aircraft mass and introduce the
gross takeoff weight constraint
[aircraft, wing, fuselage, hTail, vTail, payload, designprob] = ...
    addWeightAndSizing(aircraft, wing, fuselage, hTail, vTail, payload, designprob);


% To compute the static stability derivatives, create an instance of the Aero.FixedWing
and Aero.FixedWing.State objects
[myAircraft, CruiseState] = createFixedWing(aircraft.Mass, wing, hTail, initialValues);


% Add the static stability constraints to the optimization problem
[aircraft, wing, vTail, designprob] = ...
    addStability(aircraft, wing, fuselage, hTail, vTail, payload, designprob,
myAircraft, CruiseState);


% Estimate takeoff performance and include maximum takeoff distance, or ground roll,
constraint
[aircraft,designprob] = addPerformance(aircraft, wing.PlanformArea, wing.MeanChord,
designprob);


% Write the objective function to match the SAE Aero Design Regular Class flight score.
Units are converted to metric.
designprob.Objective = (3*(payload.Full.Mass)* (11/ (((fuselage.mass +
aircraft.Avionics.Mass + payload.Empty.Mass -1)^4) +8.9)) + 20 - 2*wing.HalfSpan*3.28);
```

```
% Let the solver run to completion by setting the maximum number of function
evaluations and iterations to infinity
options = optimoptions(designprob);
options.MaxFunctionEvaluations = Inf;
options.MaxIterations = Inf;


% If steps become too small, stop the optimization early
options.StepTolerance = 1e-04;


% Have the solver automatically plot the results of each iteration while it runs
options.PlotFcn = {'optimplotfvalconstr'};


% Use a parallel pool to speed up the computation.
options.UseParallel = false;
options.Display = 'off';


% Solving the problem returns both the maximum flight score for this design and the
corresponding values of the 12 optimization variables
[finalValues, maxScore] = solve(designprob, initialValues, 'Options', options)
```

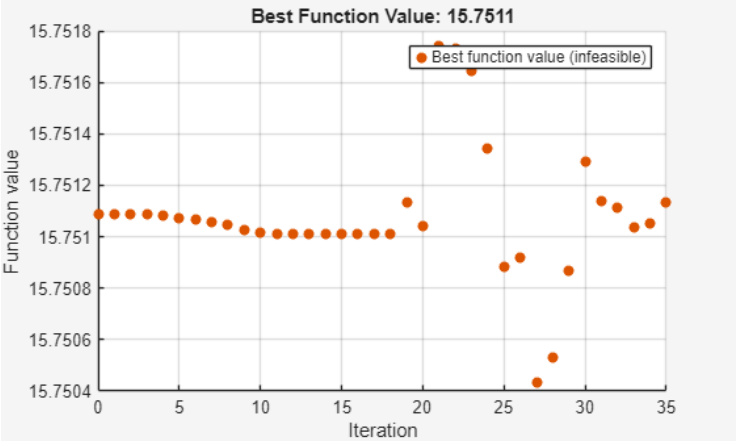


```
finalValues = struct with fields:
      P_full: 5.2867e-05
         X_p: 0.8478
         X_w: 0.3806
        b_ht: 0.2832
        b_vt: 0.1017
         b_w: 0.6477
        c_ht: 0.2238
        c_vt: 0.1300
        cr_w: 1.0603
    f_Weight: 6.8921
         l_f: 1.1615
    lambda_w: 0.9944
maxScore = 15.7511
```

Appendix C - Technical Data Sheet

Team Name: AeroJacks

School Name: Northern Arizona University

Team Number: 327

The following figures illustrate both Neutral Point and Center of Gravity as well as Static Margin against varying AOA increasing from -10° to 15°. From the graphs, there is no change in any of these values against the angle of attack. This is achievable fully through bladder construction. The bladder is designed with three baffles, the middle section being a full 1-liter volume. These containers don't directly pour into each other, instead have a top overflow port that transports water from the central container to the front and back. When half of the payload is applied to the container, 1-liter, all of the liquid water is to fill up the center section and not overflow to the other section until the plane reaches a 30° AOA. With this design, the team can fly with the 1L or 2L while maintaining the same CG.

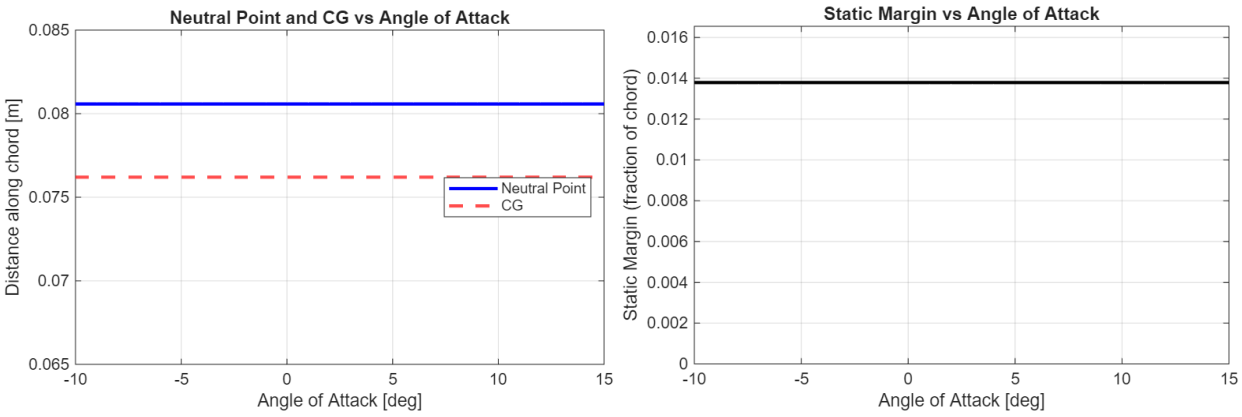

FIGURE 34: FLIGHT STABILITY AT VARYING AOA

Appendix D – Manufacturing Plan

	Manufacturing Plan (Per Plane)					
SubAssembly	Item #	Description	Material	Method	Qty	Time (hr)
Fuselage	A1.1	Nose Cone	PLA	3-D Print, sink nut inserts	1	6
	A1.2	Boom Adapter	PLA	3-D Print, sink nut inserts	1	3
	A1.3	Fuselage	Carbon Fiber	Cut with Chopsaw and Dremel	1	1
	A1.4	Payload Container	PLA	3-D Print	1	1
	A1.5	Bladder Bolts	PLA	3-D Print, add o-rings	2	0.75
	A1	**Fuselage Assembly**	Varies	Bolt together all parts	1	0.75
Main Wings	A2.1	Ailerons	PLA	3-D Print, add control horns	2	5
	A2.2	Servo Mount	PLA	3-D Print	2	0.5
	A2.3	Wing Mount	PLA	3-D Print	1	2
	A2.4	Mounting Foil	PLA	3-D Print	1	2
	A2.5	Main Wing Airfoils	Balsa	Laser Cut	8	0
	A2.6	Trailing Edge	Balsa	Laser Cut	1	0.25
	A2.7	Leading Edge	Cardstock	Cut with scissors	1	0.25
	A2.8	Spar Coupler	PLA	3-D Print	4	0.5
Empennage/Wings	A2.9	Spars	Caron Fiber	Cut with Chopsaw	6	0.25
	A2	**Main Wing Assembly**	Varies	Glue Skeleton, Wrap with Ultracote	1	8
Empennage	A3.1	Empennage Airfoils	Balsa	Laser Cut	6	0
	A3.2	Boom	Carbon Fiber	Cut with Chopsaw	1	0.25
	A3.3	Empennage Adapter	PLA	3-D Print	1	3
	A3.4	Rudder	PLA	3-D Print, add control horns	1	1
	A3.5	Elevator	Depron	Cut and shave foam, add control horns	1	2.5
	A3	**Empennage Assembly**	Varies	Attach horz. and vert. empennage	1	2.5
Landing Gear	A4.1	Nose Gear	Aluminum	Ordered	1	0
	A4.2	Main Gear	Carbon Fiber	Ordered, drill mounting holes	1	0
	A4.3	Nose Gear Bracket	PLA	3-D Print	1	0.5
	A4.4	Main Gear Bracket	PLA	3-D Print	1	0.5
	A4	**Landing Gear Assembly**	Varies	Piece together parts	1	0.25
Wiring	A5.1	Battery Mount	Velcro	Install tape on battery and fuselage	1	0.25
	A5.2	ESC Mount	Velcro	Install tape on battery and fuselage	1	0.25
	A5.3	Red Arming Plug	Cable	Install mount into fuselage	1	0.25
	A5.4	On/Off Switch	Plastic	Install mount into fuselage	1	0.25
	A5	Wiring Assembly	Varies	Tape wires on fuselage and install all connections	1	2
		Full Assembly	Varies	Fit together all subassemblies	1	1.5
		Total Assembly Time:				21.5
		Total Print time:				25.75
		Total:				47.25

Appendix E - 2-D Drawing

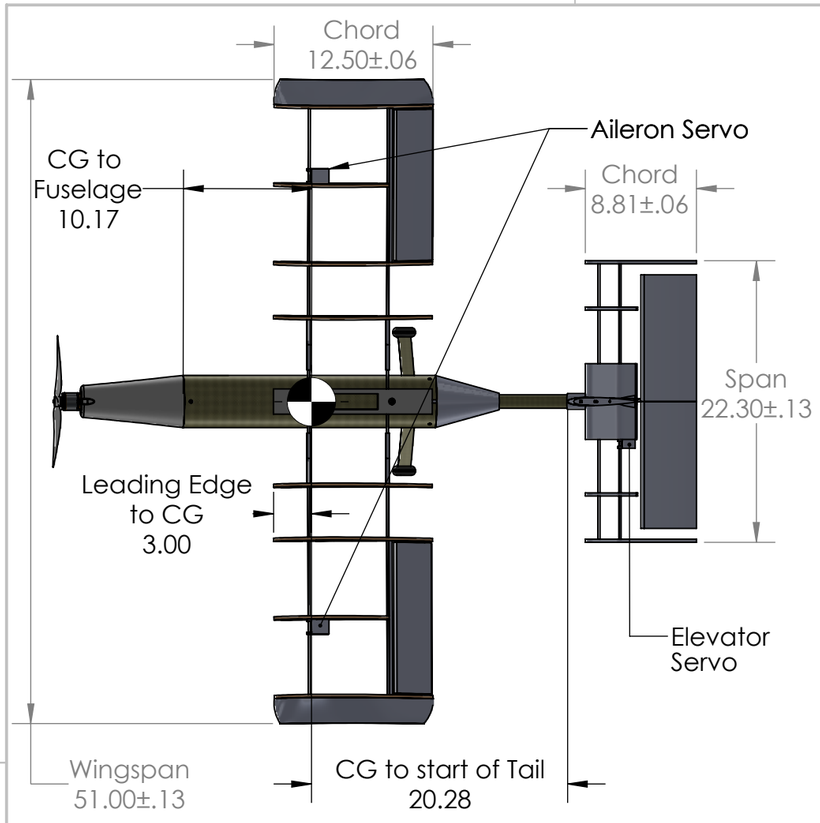

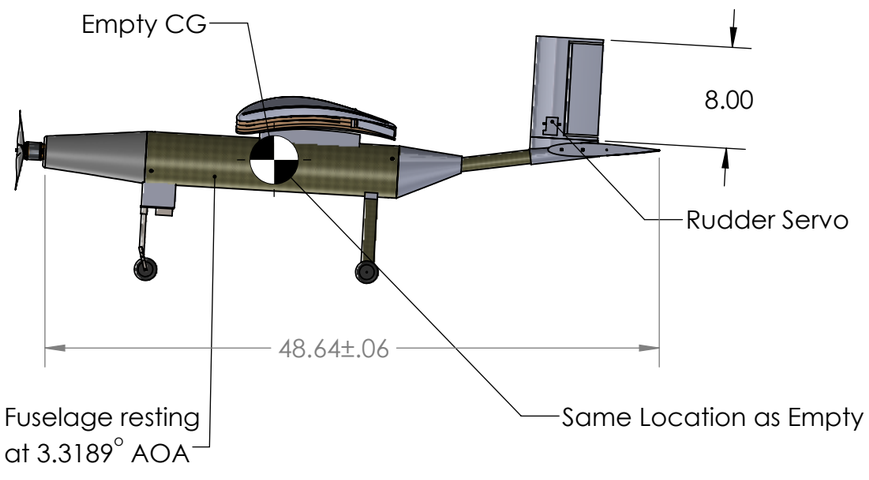

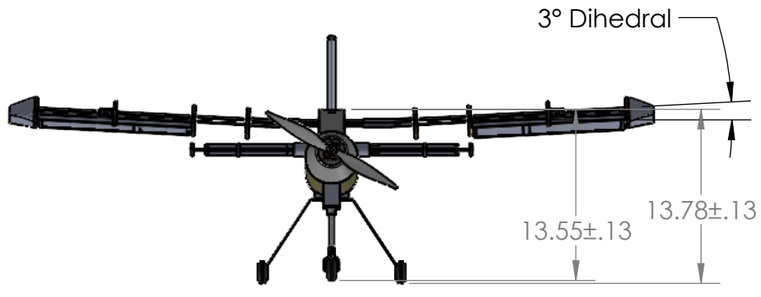

Weight and Balance			
	Weight (lbf)	Planform Distance from Datum (in)	Resultant Moment (lbf*in)
Motor	0.31	19.5	6.045
Receiver Battery	0.35	0.1	0.035
Propulsion Battery	0.72	15.38	11.0736
ESC	0.23	11.63	2.6749
Receiver	0.031	8	0.248
Servo	.025	1	0.025
Gyro	.025	0.1	0.0025
Payload	0.2	0	0

Summary Data	
Wingspan	51.02 in
Wing Area	641.58 in^2
Aspect Ratio	4
Empty Weight	7.8 lbf
Propulsion and Servo Battery Capacity	5,000 mAh | 3S | 50C
Receiver Battery	2200 mAh | 2S | 10C
Motor Make Model	FLASH HOBBY D3542 Brushless Outrunner
Motor KV	1250
Propeller Details	Uxcell 12 x 6.5 in
Servo Specifications	MG90S 9g Micro Servo Motor 179 oz-in @ 4.8V
Stability	
Static Margin Empty	25%
Static Margin Loaded	24%
Mean Aerodynamic Chord	12.58 in
Wing/Empennage Foils	E423, NACA 0012

UNLESS OTHERWISE SPECIFIED:

DIMENSIONS ARE IN INCHES
TOLERANCES:
FRACTIONAL ±
ANGULAR: MACH ± BEND ±
TWO PLACE DECIMAL ±
THREE PLACE DECIMAL ±

INTERPRET GEOMETRIC TOLERANCING PER:

MATERIAL

FINISH

NEXT ASSY | USED ON

APPLICATION | DO NOT SCALE DRAWING

	NAME	DATE
DRAWN		
CHECKED		
ENG APPR.		
MFG APPR.		
Q.A.		

COMMENTS:

TITLE: Team # 327
Aero Jacks
Northern Arizona University

SIZE B | DWG. NO. Final CAD4 | REV

SCALE: 1:12 | WEIGHT: | SHEET 1 OF 1